REPORT DOCUMENTATION PAGE

AFOSR-TR-97

0536

1. AGENCY USE ONLY *(Leave blank)*	2. REPORT DATE	3. REPORT TYPE AND DATES COVERED
	August 1996	Final Technical Report 15 Aug 93 to 14 Aug 96

4. TITLE AND SUBTITLE
Characterization of Joint Nonlinear Stiffness and Damping Behavior for Inverse Dynamics of Flexible Articulated Structures

5. FUNDING NUMBERS
F49620-93-1-0462

6. AUTHOR(S)
Assoc. Prof. Brad Paden
Thomas A. Trautt

7. PERFORMING ORGANIZATION NAME(S) AND ADDRESS(ES)
Dept of Mechanical & Environmental Engineering
University of California, Santa Barbara
Santa Barbara, CA 93106-5070

8. PERFORMING ORGANIZATION REPORT NUMBER

9. SPONSORING/MONITORING AGENCY NAME(S) AND ADDRESS(ES)
AFOSR/NA
110 Duncan Avenue, Rm B115
Bolling AFB, DC 20332-8050

10. SPONSORING/MONITORING AGENCY REPORT NUMBER
F49620-93-1-0462

11. SUPPLEMENTARY NOTES

12a. DISTRIBUTION AVAILABILITY STATEMENT
Approved for Public Release; Distribution Unlimited.

12b. DISTRIBUTION CODE

13. ABSTRACT *(Maximum 200 words)*

An inverse dynamics algorithm is derived for active vibration quenching of structures. The algorithm uses frequency domain techniques to compute an input function needed to produce a desired response at a particular degree of freedom. The desired response is a transition from the initial vibrating condition to a non-vibration condition. The algorithm can also be used to modify the input function to correct for system disturbances while the input function is already being applied to the system.

The algorithm is demostrated in a simulation of a simply supported beam controlled by a torque actuator at one end of the beam. The finite element method is used to discretized the equations of motion of the beam.

14. SUBJECT TERMS

15. NUMBER OF PAGES
10

16. PRICE CODE

17. SECURITY CLASSIFICATION OF REPORT	18. SECURITY CLASSIFICATION OF THIS PAGE	19. SECURITY CLASSIFICATION OF ABSTRACT	20. LIMITATION OF ABSTRACT
Unclassified	Unclassified	Unclassified	UL

Final Technical Report
Air Force Office of Scientific Research
Grant Number F49620-93-1-10462

Research Topic: Characterization of Joint Nonlinear Stiffness and Damping Behavior for Inverse Dynamics of Flexible Articulated Structures.

Principal Investigator: Brad Paden

Student: Thomas A. Trautt

Student's Progress for the Period August 1993 to August 1996:

The student has completed a Ph.D. in Mechanical Engineering and a Master of Arts in Applied Mathematics. The title of the dissertation for the Ph.D. is "Inverse Dynamics of Flexible Articulated Structures with Non-Zero Initial Conditions." Technical papers completed and in progress are listed below.

Paper presented at conference:

Trautt, T. A. and Bayo, E., "Active Vibration Quenching using Inverse Dynamics", *Proceedings of the 1995 Design Engineering Technical Conferences,* ASME, DE-Vol. 84-3, Vol. 3, Part C, PP. 239-246, September, 1995.

Paper published:

Trautt, T. A. and Bayo, E., "Inverse Dynamics of Non-Minimum Phase Systems with Non-Zero Initial Conditions," *Journal of Dynamics and Control,* vol. 7, pp. 49-71, 1997.

Paper submitted for publication:

Trautt, T. A. and Bayo, E., "Active Vibration Quenching of Structures using Inverse Dynamics," submitted to the *Journal of Sound and Vibration.*

Paper in progress:

Trautt, T. A. and Bayo, E., "Inverse Dynamics of Flexible Manipulators with Coulomb Friction or Backlash and Non-Zero Initial Conditions."

DE-Vol. 84-3, 1995 Design Engineering Technical Conferences
Volume 3 — Part C
ASME 1995

ACTIVE VIBRATION QUENCHING USING INVERSE DYNAMICS

Thomas A. Trautt
Department of Mechanical Engineering
University of California
Santa Barbara, California

Eduardo Bayo
Department of Mechanical Engineering
University of California
Santa Barbara, California

ABSTRACT

An inverse dynamics algorithm is derived for active vibration quenching of structures. The algorithm uses frequency domain technicques to compute an input function needed to produce a desired response at a particular degree of freedom. The desired response is a transition from the initial vibrating condition to a non-vibrating condition. The algorithm can also be used to modify the input function to correct for system disturbances while the input function is already being applied to the system.

The algorithm is demostrated in a simulation of a simply supported beam controlled by a torque actuator at one end of the beam. The finite element method is used to discretize the equations of motion of the beam.

1. INTRODUCTION

Active vibration quenching may be useful for structures where passive damping is not practical such as space based structures. Inverse dynamics may be applicable to active vibration quenching of such structures. Inverse dynamics of structures is the process of determining load profiles to produce a given displacement profile as a function of time at some point of a structure. Forward dynamics is the process of finding displacements given the loads. Forward dynamics is much simpler than inverse dynamics because it is causal whereas inverse dynamics may be non–causal. Because forward dynamics problems are causal, they can be solved by integrating forward in time. Many numerical integration schemes are available for the forward dynamics problem. In the non-causal problem encountered in inverse dynamics, the load profile to be computed begins before the known displacement profile begins so the solution cannot be determined by integrating forward in time. Inverse dynamics requires methods which look both forward and backward in time. One method which has been used for integrating in both directions in time is to use frequency domain techniques involving Fourier transforms. Another method is to use convolution integrals in the time domain. A third method is to separate the system into causal and non-causal components and integrate the non-causal component backwards in time and the causal component forward in time.

Most of the research in inverse dynamics has been for applications in controling flexible robot arms. Bayo (1987) introduced the inverse dynamics method with frequency domain techniques for open loop control of a single-link flexible robot. The position of the tip of the flexible link was controlled by a torque actuator at the pinned end of the link. The problem was solved for the link initially at rest. The method was validated experimentally by Bayo, Movaghar, and Medus (1988). A similar method presented by Bayo and Moulin (1989) was solved in the time domain by converting the Fourier transform equation into a convolution integral.

Chapnik, Heppler, and Aplevich (1993) used inverse dynamics with frequency domain techniques to control the impact response of a flexible link.

Lopez-linares et al. (1991) used inverse dynamics with frequency domain techniques and feedback to control a flexible link. Inverse dynamics was used to compute feed forward torques with the link initially at rest and feedback control was used to correct for initial conditions and disturbances. Kwon and Book (1990) presented a similar approach using a combination of inverse dynamics and feedback control. The inverse dynamics was computed by separating the system equations into causal and non-causal components.

Inverse dynamics has also been used for multibody flexible manipulators. Bayo, Papadopoulos, and Stubbe (1989) and Ledesma and Bayo (1993) solved multibody problems with the

system initially at rest. Paden et al. (1993) used inverse dynamics and feedback to control a multibody flexible manipulator. The inverse dynamics was computed for the system initially at rest and the feedback control was used to correct the trajectories for initial conditions and disturbances.

Jayasuriya and Choura (1990) presented a method for vibration quenching which was demonstrated on a pinned-pinned beam with a single fixed point actuator. The forcing function was a sum of sines and cosines at the natural frequencies of the system. The coefficients to the sines and cosines were determined so that all the displacements and velocities were zero at some future time. This method controls the structure at the end point of a time interval as in the slewing problem whereas the inverse dynamics methods mentioned above control a degree of freedom through a predetermined trajectory during a time interval.

In the present paper, inverse dynamics is used to quench vibrations in a pinned-pinned beam. A torque actuator acts on one end of the beam to control the angular deflection at the other end of the beam. The beam is modeled with the same physical properties as modeled by Jayasuriya and Choura. The equations of motion are discretized using finite element methods assuming Bernouli-Euler beam theory. An inverse dynamics algorithm is derived using frequency domain techniques. The algorithm is demonstrated in computer simulations of vibration quenching of the pinned-pinned beam. Three problems are demonstrated. The first problem is to quench the beam when only the first vibration mode is active. The second problem is to quench the beam when many modes are active. In the third problem, a disturbance is added to the system after the forcing function is initiated, and the forcing function is then changed to compensate for the disturbance. The ability of the algorithm to correct the forcing function may lead to the ability for real time control by continually updating the forcing function.

2. MODELING

The inverse dynamics algorithm will be demonstrated in a simulation of a pinned-pinned beam as shown in Figure 1. A torque, $f(t)$, as a function of time, t, acts on the left end of the beam to control the angular displacement at the right end of the beam. The beam has a total length L, Young's modulus E, constant cross section area A, constant area moment of inertia I, and density ρ.

We will use finite element methods to discretize the equations of motion. We assume Bernoulli-Euler beam theory and small deflections, and neglect gravity, rotory inertia, and axial loading. A typical element is shown in Figure 2. Let $v(s,t)$ be the tranverse displacement as a function of time, t, and distance, s, along the element. Let $\mathbf{v}$ be the nodal displacements and $\mathbf{u}$ be the corresponding nodal loads applied to the element. The potential energy of the element is

$$V = \frac{1}{2}\int_0^{L_e} EI\left[v''(s,t)\right]^2 ds \tag{1}$$

where the primes denote partial derivatives with respect to s and L_e is the length of the element. The virtual work done by inertia forces is

$$\delta W_{inertia} = \int_0^{L_e} \delta v[-\rho A\ddot{v}(s,t)]ds \tag{2}$$

where the dots denote partial derivatives with respect to time. The virtual work done by nonconservative forces is

$$\delta W_{nc} = \delta \mathbf{v}^T \mathbf{u} \tag{3}$$

The principle of virtual work can be stated

$$-\delta W_{inertia} + \delta V - \delta W_{nc} = 0 \tag{4}$$

Substituting equations (1), (2), and (3) into this equation, we obtain

$$\int_0^{L_e} \rho A\delta v\ddot{v}(s,t)ds + \int_0^{L_e} EI\delta v''v''(s,t)ds - \delta \mathbf{v}^T\mathbf{u} = 0 \tag{5}$$

We discretize the displacements as follows.

$$v(s,t) = \mathbf{h}(s)\mathbf{v}(t) = \mathbf{v}^T\mathbf{h}^T \tag{6}$$

In this equation, $\mathbf{h}$ is a row vector of shape functions based on the Hermite polynomials (Meirovitch, 1990). The shape functions are

$$\begin{aligned} h_1(s) &= L_e\left[x/L_e - 2(x/L_e)^2 + (x/L_e)^3\right] \\ h_2(s) &= L_e\left[-(x/L_e)^2 + (x/L_e)^3\right] \\ h_3(s) &= 1 - 3(x/L_e)^2 + 2(x/L_e)^3 \\ h_4(s) &= 3(x/L_e)^2 - 2(x/L_e)^3 \end{aligned} \tag{7}$$

From equation (6) we can derive the following expressions.

$$\begin{aligned} \delta v &= \delta \mathbf{v}^T\mathbf{h}^T \\ \ddot{v} &= \mathbf{h}\ddot{\mathbf{v}} \\ \delta v'' &= \delta \mathbf{v}^T(\mathbf{h}'')^T \\ v'' &= \mathbf{h}''\mathbf{v} \end{aligned} \tag{8}$$

Substituting equations (8) into equation (5), we obtain

$$\delta \mathbf{v}^T\left[\rho A\int_0^{L_e} \mathbf{h}^T\mathbf{h}ds\ddot{\mathbf{v}} + EI\int_0^{L_e} (\mathbf{h}'')^T\mathbf{h}''ds\mathbf{v} - \mathbf{u}\right] = 0 \tag{9}$$

Setting the part in the brackets equal to zero, we obtain

$$\mathbf{M}_e\ddot{\mathbf{v}} + \mathbf{K}_e\mathbf{v} = \mathbf{u} \tag{10}$$

where

$$\mathbf{M}_e = \rho A\int_0^{L_e} \mathbf{h}^T\mathbf{h}ds \tag{11}$$

and

$$\mathbf{K}_e = EI\int_0^{L_e} (\mathbf{h}'')^T\mathbf{h}ds \tag{12}$$

The matrices $\mathbf{M}_e$ and $\mathbf{K}_e$ are the mass and stiffness matrices respectively for an element. The beam is modeled with several elements as shown in Figure 3. Assembling the elements we obtain the matrix equation of motion for the system,

$$\mathbf{M}\ddot{\mathbf{y}} + \mathbf{K}\mathbf{y} = \mathbf{b}f(t) \tag{13}$$

where **M** is the system mass matrix, **K** is the system stiffness matrix, **y** is a vector of degrees of freedom, and **b** is a loading vector with a unit value at the degree of freedom at which the torque is applied and zeros in the rest of the vector.

We add Rayleigh damping to the system using the expression

$$\mathbf{C} = \alpha\mathbf{M} + \beta\mathbf{K} \tag{14}$$

where **C** is the damping matrix, and α and β are constants. The matrix equation of motion of the system with damping becomes

$$\mathbf{M}\ddot{\mathbf{y}} + \mathbf{C}\dot{\mathbf{y}} + \mathbf{K}\mathbf{y} = \mathbf{b}f(t) \tag{15}$$

The damping ratio at each natural frequency can be calculated from

$$\zeta_i = \frac{1}{2}\left(\frac{\alpha}{\omega_i} + \beta\omega_i\right) \tag{16}$$

where ζ_i is the damping ratio and ω_i is the natural frequency in radians per unit time.

3. INVERSE DYNAMICS

We want to solve for the torque profile, $f(t)$, which will quench the initial vibrations in the system. Taking the Fourier transform of equation (15), we obtain

$$(-\omega^2\mathbf{M} + i\omega\mathbf{C} + \mathbf{K})\hat{\mathbf{y}}(\omega) = \mathbf{b}\hat{f}(\omega) \tag{17}$$

or

$$\hat{\mathbf{A}}\hat{\mathbf{y}} = \mathbf{b}\hat{f} \tag{18}$$

where

$$\hat{\mathbf{A}}(\omega) = (-\omega^2\mathbf{M} + i\omega\mathbf{C} + \mathbf{K}) \tag{19}$$

The caret denotes the Fourier transform and ω is frequency in radians per unit time. Solving equation (18) for $\hat{\mathbf{y}}$, we obtain

$$\hat{\mathbf{y}} = \hat{\mathbf{g}}\hat{f} \tag{20}$$

where

$$\hat{\mathbf{g}} = \hat{\mathbf{A}}^{-1}\mathbf{b} = (-\omega^2\mathbf{M} + i\omega\mathbf{C} + \mathbf{K})^{-1}\mathbf{b} \tag{21}$$

Without damping in the system, matrix **A** would not be invertible when ω is equal to a natural frequency. For this reason, it is necessary to have some damping in the system for the algorithm to be usable.

We can write equation (20) in an expanded form as follows.

$$\begin{pmatrix} \hat{y}_1 \\ \vdots \\ \hat{y}_n \end{pmatrix} = \begin{pmatrix} \hat{g}_1 \\ \vdots \\ \hat{g}_n \end{pmatrix} \hat{f} \tag{22}$$

The kth equation corresponding to the controlled degree of freedom, y_k, gives us

$$\hat{y}_k = \hat{g}_k\hat{f} \tag{23}$$

Solving for $\hat{f}$, we obtain

$$\hat{f} = \hat{y}_k / \hat{g}_k \tag{24}$$

We need to define a profile for $y_k(t)$ which will cancel the vibrations due to the initial conditions. We also need the profile to be finite in time so that we can compute its fast Fourier transform (FFT). To cancel the vibrations for a finite time, we need the profile to be the negative of the homogeneous response for a finite time. Therefore, we create a windowed profile, $z(t)$, as follows.

$$z(t) = -w(t)\, y_k(t) \tag{25}$$

where $w(t)$ is a windowing function and $y_k(t)$ is the homogeneous response to the initial conditions. The homogeneous response can be computed using numerical integration. The general shape of the windowing function and its first two derivatives are shown in Figure 4. The time from t_0 to t_f is the window of time for the FFT computation. We will go into more detail on the windowing function later in our discussion. We compute the FFT of $z(t)$ and substitute it for $\hat{y}_k$ in equation (24) to obtain

$$\hat{f} = \hat{z} / \hat{g}_k \tag{26}$$

where $\hat{g}_k$ is computed at the same frequencies used to compute the FFT. Taking the inverse fast Fourier transform (IFFT) of $\hat{f}(\omega)$, we obtain the torque profile, $f(t)$. We can think of $f(t)$ as a composition of two parts. The first part cancels the vibration and the second part causes the system to transition back to the vibrating condition. We need to eliminate the part of the forcing function which causes the system to transition back to the vibrating condition. We do this by eliminating the second half of $f(t)$ as follows.

$$f_2(t) = \begin{cases} f(t) & , \ t_0 \le t \le t_m \\ 0 & , \ t_m < t \end{cases} \tag{27}$$

In this formula, t_0 is the starting time for the FFT window, t_m is the midpoint of the FFT window, and $f_2(t)$ is the desired forcing function which will cancel the vibrations. There will be some error due to truncation and overlap of the two parts of the torque profile, $f(t)$. This error can be made negligible by choosing large enough time spans in the windowing function. In the time spans where $z(t)$ is following a homogeneous response, the torque profile approaches zero as the rest of the system approaches the homogeneous response.

We may want to modify the forcing function while it is being applied to correct for disturbances in the system. We assume we already have a forcing function, $f_1(t)$, which will produce a profile of $y_k(t)$ which will follow a homogenous response after a time t_2 and has zero force after t_m. The forcing function, $f_2(t)$ from equation (27) will have these properties.

Using numerical integration, we compute the response of $y_k(t)$ due to initial conditions and the forcing function from

$$\mathbf{M}\ddot{\mathbf{y}} + \mathbf{C}\dot{\mathbf{y}} + \mathbf{K}\mathbf{y} = \mathbf{b}f_1(t) \tag{28}$$

The windowed profile is then computed from

$$z(t) = -w(t)\, y_k(t) \tag{29}$$

We compute $\hat{g}_k(\omega)$ at discrete frequencies using the following equation.

$$\hat{\mathbf{g}} = (-\omega^2\mathbf{M} + i\omega\mathbf{C} + \mathbf{K})^{-1}\mathbf{b} \tag{30}$$

We compute the FFT of $z(t)$ and then solve for $\hat{f}$ from

$$\hat{f} = \hat{z} \,/\, \hat{g}_k \tag{31}$$

We compute the IFFT of $\hat{f}(\omega)$ to obtain $f(t)$ and add the first half of $f(t)$ to $f_1(t)$ to obtain the new desired forcing function, $f_2(t)$.

$$f_2(t) = \begin{cases} f(t) + f_1(t) \;, & t_0 \le t \le t_m \\ 0 \;, & t_m < t \end{cases} \tag{32}$$

Using numerical integration we can compute the new response of the system from

$$\mathbf{M}\ddot{\mathbf{y}} + \mathbf{C}\dot{\mathbf{y}} + \mathbf{K}\mathbf{y} = \mathbf{b}f_2(t) \tag{33}$$

Equations (28) through (33) summarize the algorithm. The algorithm can be continually repeated by using the profile of $f_2(t)$ or a portion of $f_2(t)$ with an apropriate time shift substituted for $f_1(t)$ in equation (28).

The derivation of the windowing function, $w(t)$, follows. We want $w(t)$ to produce smooth functions of z, $\dot{z}$ and $\ddot{z}$ so that the resulting torque profile, $f(t)$, is also smooth. For $\dddot{z}$ to be smooth, we need $\ddddot{z}$ to be continuous. The windowed profile and its derivatives are

$$\begin{aligned} z &= -w\, y_k \\ \dot{z} &= -\dot{w}\, y_k - w\, \dot{y}_k \\ \ddot{z} &= -\ddot{w}\, y_k - 2\dot{w}\, \dot{y}_k - w\, \ddot{y}_k \\ \dddot{z} &= -\dddot{w}\, y_k - 3\ddot{w}\, \dot{y}_k - 3\dot{w}\, \ddot{y}_k - w\, \dddot{y}_k \end{aligned} \tag{34}$$

The windowing function, $w(t)$, transitions from zero to one between t_1 and t_2. For z, $\dot{z}$ and $\ddot{z}$ to be smooth at t_1 and t_2, we have the following requirements on $w(t)$.

$$\begin{aligned} &w(t_1) = \dot{w}(t_1) = \ddot{w}(t_1) = \dddot{w}(t_1) = 0 \\ &w(t_2) = 1 \\ &\dot{w}(t_2) = \ddot{w}(t_2) = \dddot{w}(t_2) = 0 \end{aligned} \tag{35}$$

Between times t_1 and t_2, we let $w(t)$ be described by a polynomial, $p(\theta)$.

$$w(t) = p(\theta) \tag{36}$$

where

$$\theta = \frac{t - t_1}{t_2 - t_1} \tag{37}$$

Then, $p(\theta)$ will have the following requirements.

$$\begin{aligned} &p(0) = p'(0) = p''(0) = p'''(0) = 0 \\ &p(1) = 1 \\ &p'(1) = p''(1) = p'''(1) = 0 \end{aligned} \tag{38}$$

The primes denote derivatives with respect to θ. We have eight constraints on $p(\theta)$ so we need a polynomial with eight constants. The polynomial, $p(\theta)$, and its derivatives can be written as

$$\begin{aligned} p(\theta) &= a_0 + a_1\theta + a_2\theta^2 + a_3\theta^3 + a_4\theta^4 + a_5\theta^5 + a_6\theta^6 + a_7\theta^7 \\ p'(\theta) &= a_1 + 2a_2\theta + 3a_3\theta^2 + 4a_4\theta^3 + 5a_5\theta^4 + 6a_6\theta^5 + 7a_7\theta^6 \\ p''(\theta) &= 2a_2 + 6a_3\theta + 12a_4\theta^2 + 20a_5\theta^3 + 30a_6\theta^4 + 42a_7\theta^5 \\ p'''(\theta) &= 6a_3 + 24a_4\theta + 60a_5\theta^2 + 120a_6\theta^3 + 210a_7\theta^4 \end{aligned} \tag{39}$$

where a_0 through a_7 are constants. From the requirements $p(0)=p'(0)=p''(0)=p'''(0)=0$, we obtain

$$a_0 = a_1 = a_2 = a_3 = 0 \tag{40}$$

From the other four requirements we obtain

$$\begin{aligned} &a_4 + a_5 + a_6 + a_7 = 1 \\ &4a_4 + 5a_5 + 6a_6 + 7a_7 = 0 \\ &12a_4 + 20a_5 + 30a_6 + 42a_7 = 0 \\ &24a_4 + 60a_5 + 120a_6 + 210a_7 = 0 \end{aligned} \tag{41}$$

or in matrix form

$$\begin{bmatrix} 1 & 1 & 1 & 1 \\ 4 & 5 & 6 & 7 \\ 12 & 20 & 30 & 42 \\ 24 & 60 & 120 & 210 \end{bmatrix} \begin{bmatrix} a_4 \\ a_5 \\ a_6 \\ a_7 \end{bmatrix} = \begin{bmatrix} 1 \\ 0 \\ 0 \\ 0 \end{bmatrix} \tag{42}$$

The solution to these equations is

$$\begin{bmatrix} a_4 \\ a_5 \\ a_6 \\ a_7 \end{bmatrix} = \begin{bmatrix} 35 \\ -84 \\ 70 \\ -20 \end{bmatrix} \tag{43}$$

and we obtain the polynomial

$$p(\theta) = -20\theta^7 + 70\theta^6 - 84\theta^5 + 35\theta^4 \tag{44}$$

where

$$\theta = \frac{t - t_1}{t_2 - t_1} \;, \qquad t_1 \le t \le t_2 \tag{45}$$

Between t_3 and t_4, we can use $p(\phi)$ where ϕ is given by the following expression which will give us a transition from one back to zero.

$$\phi = \frac{t_4 - t}{t_4 - t_3} \;, \qquad t_3 \le t \le t_4 \tag{46}$$

Putting the pieces of $w(t)$ together, we obtain the following formula.

$$w(t) = \begin{cases} 0, & t_0 \le t \le t_1 \\ p(\theta(t)), & t_1 \le t \le t_2 \\ 1, & t_2 \le t \le t_3 \\ p(\phi(t)), & t_3 \le t \le t_4 \\ 0, & t_4 \le t \le t_f \end{cases} \quad (47)$$

This formula was used to make the plots of w, $\dot{w}$, and $\ddot{w}$ shown in Figure 4.

4. APPLICATION

The inverse dynamics algorithm will be demonstrated in a computer simulation of a pinned-pinned beam as shown in Figure 1. The beam is modeled with six finite elements and has the following properties:

$L = 0.762$ m = total length
$A = 1.613 \times 10^{-5}$ m^2 = cross sectional area
$I = 9.6361 \times 10^{-13}$ m^4 = area moment of inertia
$\rho = 2710$ kg/m^3 = density
$E = 71 \times 10^9$ N/m^2 = Young's modulus
$\alpha = .01$/sec, $\beta = .0001$ sec, Rayleigh damping constants (48)

The windowing function, $w(t)$, shown in Figure 4 will have the following values for t_0 through t_f.

$t_0 = 0.0$ sec
$t_1 = 0.1$ sec
$t_2 = 0.2$ sec
$t_m = 0.3$ sec
$t_3 = 0.4$ sec
$t_4 = 0.5$ sec
$t_f = 0.6$ sec (49)

The first six natural frequencies of the discretized system are

$\omega_1 = 3.38$ Hz $= 21.2$ rad/sec
$\omega_2 = 13.5$ Hz $= 84.8$ rad/sec
$\omega_3 = 30.6$ Hz $= 192$ rad/sec
$\omega_4 = 54.7$ Hz $= 344$ rad/sec
$\omega_5 = 86.8$ Hz $= 545$ rad/sec
$\omega_6 = 135$ Hz $= 848$ rad/sec (50)

The damping ratios associated with the first six natural frequencies are

$\zeta_1 = .0013$
$\zeta_2 = .0043$
$\zeta_3 = .0096$
$\zeta_4 = .017$
$\zeta_5 = .027$
$\zeta_6 = .042$ (51)

We can see that this system is very lightly damped at the lower frequencies.

The inverse dynamics algorithm will be demonstrated on three problems. The first problem is to quench the vibrations when only the first mode is active. The second problem is to quench the vibrations when many modes are active. In the third problem, a disturbance is added to the system while the torque profile is already being applied, and the inverse dynamics algorithm is used to change the torque profile to correct for the disturbance.

4.1 First Mode Active

The initial displacement profile of the beam is the first mode shape with a displacement of .075 m at the center of the beam. The initial velocities are all zero. The inverse dynamics algorithm is used to compute a torque profile which will cancel the vibrations in the beam. The response of the beam is computed using Newmark's constant-average-acceleration method (Bathe, 1982). The torque profile and displacement profiles are shown in Figure 5. Angular displacements at the right end of the beam and mid-span displacements are shown with and without the torque.

We see that the torque is at a negligible level at 0.0 second and at 0.3 second where the torque profile is truncated. These times correspond with t_0 and t_m shown in the graph of the windowing function in Figure 4.

The angular dispacement which is the controlled degree of freedom settles down by 0.2 second which corresponds with the time t_2 shown in the graph of the windowing function. The torque profile continues to damp the rest of the system for a short time after the controlled degree of freedom has already settled down. We see that the mid-span displacement settles down after the angular displacement settles down.

4.2 Many Modes Active

The initial conditions of the vectors $\mathbf{y}$ and $\dot{\mathbf{y}}$ are all zero except for an angular velocity of 10 rad/sec at the left end of the beam. These initial conditions include many vibration modes. The inverse dynamics algorithm is used to compute the torque to quench the vibrations. The torque profile and displacement profiles with and without the torque are shown in Figure 6. As in the previous problem, we see that the angular displacement settles down by 0.2 second and the mid-span displacement settles down after the angular displacement settles down.

4.3 Correct for a Disturbance

Starting with the previous solution, we add a disturbance to the torque profile from time t=0.02 second to time t=0.03

second. At time t=0.06 second, we apply the inverse dynamics algorithm to correct the torque profile. Torque profiles with the disturbance and displacement profiles are shown in Figure 7 with and without the correction.

Since the algorithm to correct the profile is started at time t=0.06, we expect the angular displacement to settle down by 0.26 second. As we see in the plot, the angular displacement does settle down by 0.26 second as expected.

5.0 CONCLUSION

An inverse dynamics algorithm for quenching vibrations has been presented. The algorithm was demonstrated analytically on a pinned-pinned beam with a torque actuator at one end and has shown good results. The vibrations are damped out quickly and the required torque profiles are smooth. The algorithm can be repeated to correct for errors and disturbances after the forcing function is initiated. This will lead to the ability for real time control by continually updating the algorithm at discrete time intervals.

The algorithm can be applied to more complicated structures. The torque or force actuator should be applied to a degree of freedom which is not a node of one of the natural frequencies. The actuator must also be non-colocated with the controlled degree of freedom. The controlled degree of freedom should not be at a node of any natural frequency which is to be quenched.

The algorithm is robust to errors in initial conditions. Because the algorithm uses superposition, we can superpose the assumed initial conditions and the error in the initial conditions. Applying the algorithm will eliminate the vibrations due to the assumed initial conditions. The response after the algorithm is applied will be the homogeneous response to the error in the initial conditions. Each time the algorithm is applied this error will be reduced.

The algorithm is also robust to errors in damping, but is not very robust to errors in mass and stiffness. Errors in mass and stiffness can cause the computed response to be out of phase with the actual response especially at the higher frequencies and we would not get the desired cancelling effect when applying the algorithm. The robustness can be improved by using inverse dynamics to compute a feed forward control and adding closed-loop tracking control to track the trajectories computed by the inverse dynamics algorithm (Kwon and Book, 1990), (Lopez-Linares et al., 1991) and (Paden et al., 1993).

More research is needed to make the computations more practical for real applications. Simpler models could be used if only the first one or two vibration modes need to be actively quenched. If we assume only the first two modes are present, then less sensors will be needed to estimate the initial conditions of the system. Simplifying the model and reducing the number of sensors would reduce the computations at the cost of losing some accuracy. The computations can also be made more efficient by using the time domain approach presented by Bayo and Moulin (1989) instead of the frequency domain approach.

ACKNOWLEDGMENTS

The authors would like to acknowledge the support of this work by the AFOSR under grant F49620-93-1-0462.

REFERENCES

Bathe, K.J., *Finite Element Procedures in Engineering Analysis*, Prentice-Hall, Englewood Cliffs, NJ, 1982, pp. 511-512.

Bayo, E., "A Finite Element Approach to Control the End-Point Motion of a Single-Link Flexible Robot," *Journal of Robotic Systems*, Vol. 4, No. 1, pp. 63-75, 1987.

Bayo, E. and Moulin, H., "An Efficient Computation of the Inverse Dynamics of Flexible Manipulators in the Time Domain," *Proceedings of IEEE Conference on Robotics and Automation*, Scottsdale, Arizona, Vol. 2, pp. 710-715, 1989.

Bayo, E., Movaghar, R., and Medus, M., "Inverse Dynamics of a Single-Link Flexible Robot, Analytical and Experimental Results," *International Journal of Robotics and Automation*, Vol. 3, No. 3, pp. 150-157, Fall 1988.

Bayo, E., Serna, M. A., Papadopoulos, P., and Stubbe, J. R., "Inverse Dynamics and Kinematics of Multi-Link Elastic Robots: an Interative Frequency Domain Approach," *International Journal of Robotics Research*, Vol. 8, No. 6, pp. 49-62, Dec. 1989.

Chapnik, B. V., Heppler, G. R. and Aplevich, J. D., "Controlling the Impact Response of A One-Link Flexible Robotic Arm," *IEEE Transactions on Robotics and Automation*, Vol. 9, No. 3, pp. 346-351, June 1993.

Jayasuriya, S. and Choura, S., "Active Quenching of a Set of Predetermined Vibratory Modes of a Beam by a Single Fixed Point Actuator," *International Journal of Control*, Vol. 51, No. 2, pp. 445-467, 1990.

Kwon, D.-S. and Book, W.J., "An Inverse Dynamic Method Yielding Flexible Manipulator State Trajectories," *Proceedings of American Control Conference*, San Diego, pp. 186-193, June 1990.

Ledesma, R. and Bayo, E., "A Non-Recursive Lagrangian Solution of the Non-Causal Inverse Dynamics of Flexible Multibody Systems: The Planar Case," *International Journal for Numerical Methods in Engineering*, Vol. 36, pp. 2725-2741, 1993.

Lopez-Linares, S., Serna, M. A., Jacobus, R. F. and Bayo, E., "An Inverse Dynamics Based Closed-Loop Trajectory Tracking Control for a Flexible Arm," *Modeling and Control of Compliant and Rigid Motion Systems*, ASME, DSC-Vol. 31, pp. 21-26, Dec. 1991.

Meirovitch, L., *Dynamics and Control of Structures*, John Wiley & Sons, New York, 1990, p. 295.

Paden, B., Chen, D., Ledesma, R., and Bayo, E., "Exponentially Stable Tracking Control for Multijoint Flexible-Link Manipulators," *ASME Journal of Dynamic Systems, Measurement, and Control*, Vol. 115, pp. 53-59, March 1993.

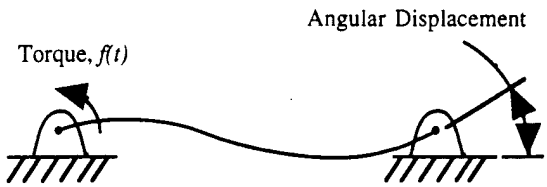

FIG. 1. PINNED-PINNED BEAM

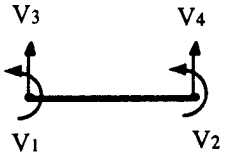

FIG. 2. BEAM ELEMENT

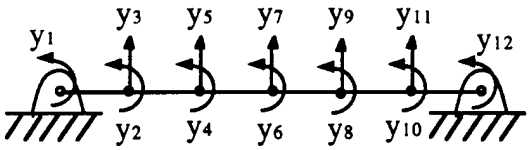

FIG. 3. FINITE ELEMENT MODEL

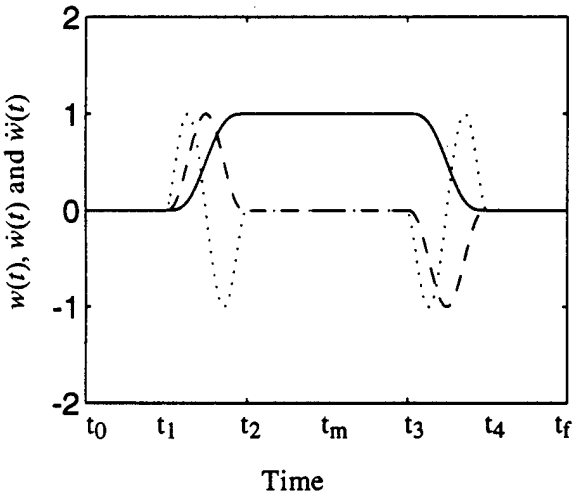

FIG. 4. WINDOWING FUNCTION, $w(t)$ (SOLID LINE), AND ITS DERIVATIVES, $\dot{w}(t)$ (DASHED LINE) AND $\ddot{w}(t)$ (DOTTED LINE), NORMALIZED TO ONE.

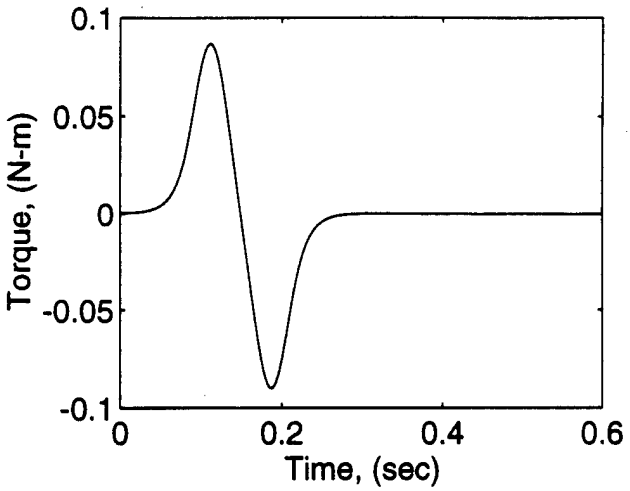

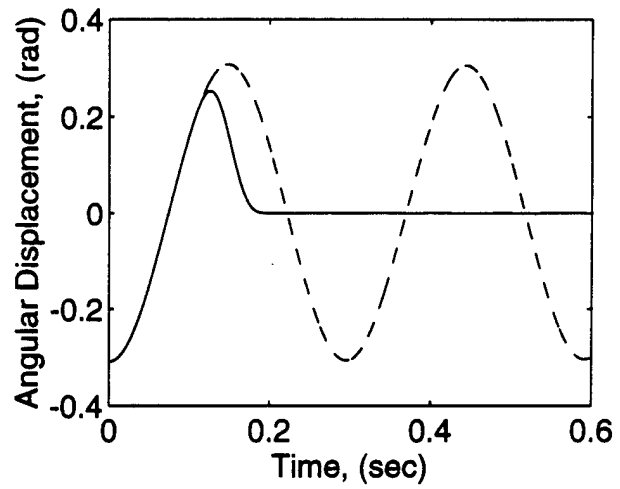

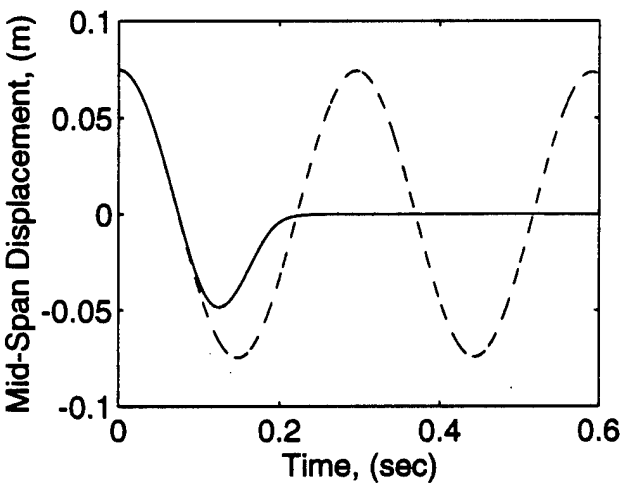

FIG. 5. FIRST MODE ACTIVE - TORQUE TO CANCEL VIBRATIONS, ANGULAR DISPLACEMENT AT RIGHT END, MID-SPAN DISPLACEMENT, WITH TORQUE (SOLID LINE), WITHOUT TORQUE (DASHED LINE).

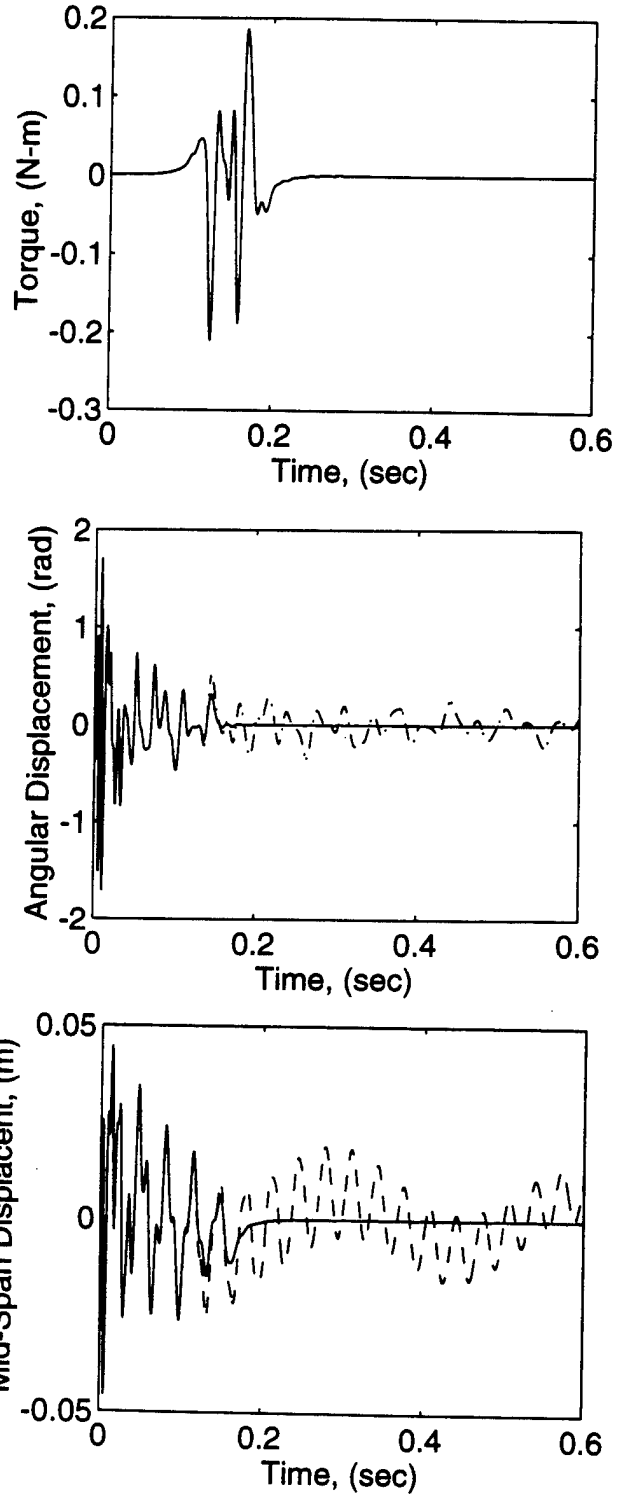

FIG. 6. MANY MODES ACTIVE - TORQUE TO CANCEL VIBRATIONS, ANGULAR DISPLACEMENT AT RIGHT END, MID-SPAN DISPLACEMENT, WITH TORQUE (SOLID LINE), WITHOUT TORQUE (DASHED LINE).

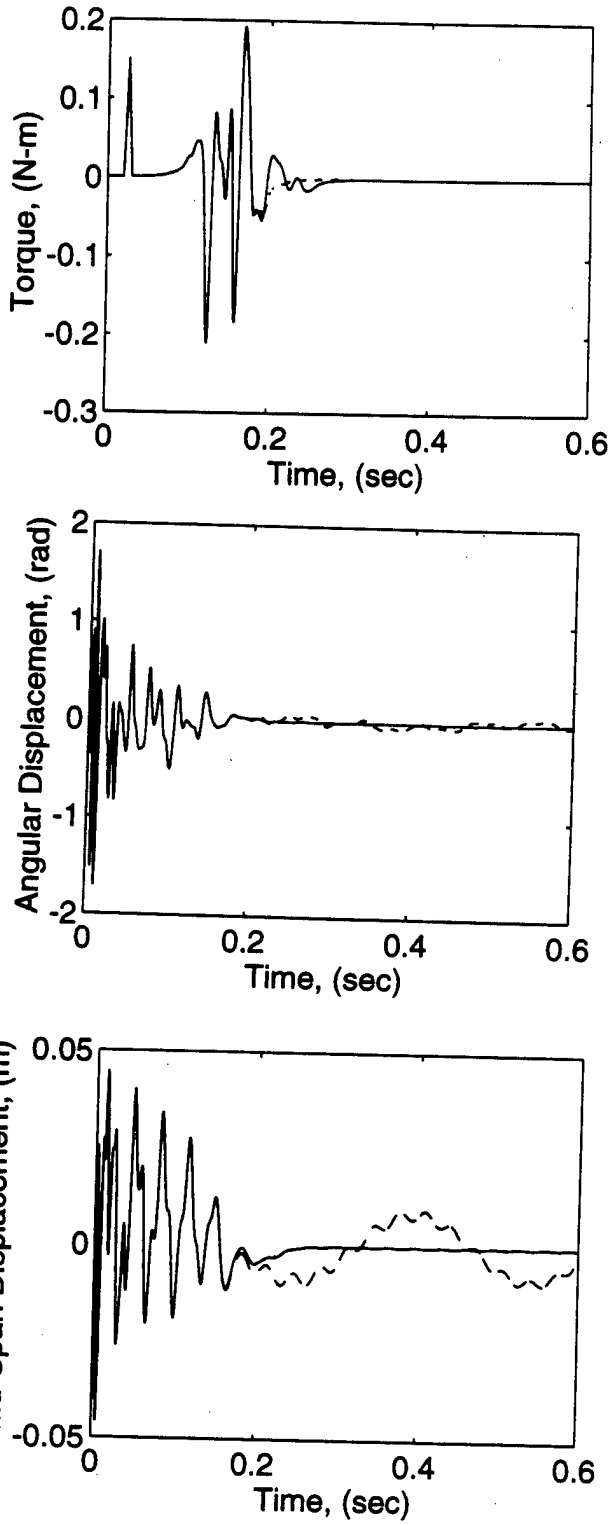

FIG. 7. DISTURBANCE IN TORQUE PROFILE - TORQUE , ANGULAR DISPLACEMENT AT RIGHT END, MID-SPAN DISPLACEMENT, WITH CORRECTION (SOLID LINE), WITHOUT CORRECTION (DASHED LINE).